A Research Report Sponsored by the Reinforced Concrete Research Council

Lateral Load Resistance of Unbonded Post-Tensioned Flat Plate Construction

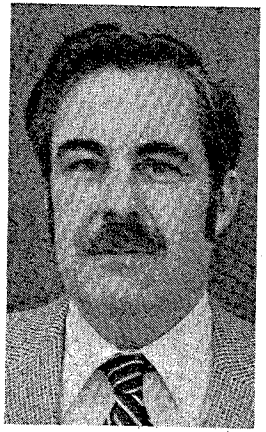

Neil M. Hawkins
Professor and Chairman
Department of Civil Engineering
University of Washington
Seattle, Washington

Synopsis

Results are described of tests to failure on six full-scale unbonded post-tensioned prestressed concrete slab-column subassemblages subjected to loadings in which reversing moments, combined with shears, were transferred between the slab and the column.

It is concluded that prestressed concrete slab-to-interior column subassemblages can be proportioned so as to behave in a ductile manner. The moment transfer strength of interior column connections can be evaluated using Sections 11.12.2 and 13.3.4 of ACI 318-77 and the lateral load stiffness can be assessed using Section 13.7 of ACI 318-77 provided the slab can be taken as uncracked due to gravity loadings.

For slab-to-exterior column connections, bonded reinforcement, detailed so that it can act as torsional reinforcement, should be provided when the upward shear stress at the discontinuous edge, evaluated using Section 11.12.2 of ACI 318-77, exceeds $2\sqrt{f'_c}$ psi ($0.17\sqrt{f'_c}$ MPa).

Two-way post-tensioned flat plate construction is commonly used for both high- and low-rise structures such as parking garages, apartments, offices and industrial buildings. Two forms of construction are used: slabs cast monolithically with columns and lift slabs. For both forms, economics and speed of construction considerations usually dictate that slabs be post-tensioned with unbonded tendons.

For moderate earthquakes and high winds, the response of a structure should be essentially elastic. For that condition, accurate information is needed on the lateral load stiffness of the flat plate frame and its attachments. For severe earthquakes or extremely high winds, the structure should be able to absorb and ultimately dissipate large amounts of energy. Under the deformations and moments caused by that condition, punching failures should not occur at plate-to-column connections. The main objective of this study was to determine the factors dictating the strength and stiffness of prestressed concrete plate-to-column connections transferring moments.

Frequently, in order to make the placement of tendons easier, banded construction, as shown in Fig. 1, is used. Many questions have been raised by the structural engineering profession concerning the behavior and safety of banded post-tensioned slabs. Therefore, examination of the behavior of connections in such slabs was one of the objectives of this study.

Service and design moments for prestressed concrete flat plates should be predicted using the Equivalent Frame Method of Section 13.7 of ACI 318-77.[1,2] Dead, live and the balanced loads caused by post-tensioning are placed on the equivalent frame. The post-tensioning force is typically determined from allowable flexural tensile stress limitations or even deflection criteria. Flexural tensile stresses are based on the average moment across the "beam" member of the equivalent frame and therefore the actual stress at a column face may be considerably higher than the calculated stress.

Plates are usually at the point of cracking at the column perimeter or are cracked under the dead weight of the slab. A minimum amount of deformed bar reinforcement is necessary in the column region to control cracking. One of the objectives of this study was to examine the adequacy for moment transfer situations of current recommendations for the amount and distribution of that reinforcement.[1]

Test Specimens

This section describes the selection of proportions of the test specimens, the test program, details of the interior column, lift slab, and edge column specimens, materials, and test setup and instrumentation.

Selection of Proportions

Proportions for the test specimens were selected after detailed examination of a typical two-way unbonded prototype flat plate structure designed by Atlas Prestressing. That structure is shown in Fig. 1. It was three bays wide in the 21 - 16 - 21-ft (6.3 - 4.8 - 6.3 m) direction and infinitely long in the 20-ft (6 m) direction. The slab was designed for a live load of 40 psf (1920 Pa) and a

Table 1. Properties of test specimens.

Slab No.	Type	Concrete strength* f'_c		Prestress				Loading	Shear kips (kN)	Moment ft-kip (m-kN)
				Transverse		Longitudinal				
		psi	MPa	Type	f_{pc} psi (MPa)	Type	f_{pc} psi (MPa)			
1	Interior	3850 (3920)	26.5 (27.0)	Bundled	160 (1.10)	Distributed	160 (1.10)	Proportionate	66.8 (300.6)	51.5 (70.7)
2	Exterior	4200 (4100)	28.9 (28.2)	Two through column	160 (1.10)	Two through column	160 (1.10)	Proportionate	30.8 (138.6)	37.0 (50.8)
3	Interior	3650 (3900)	25.1 (26.9)	Distributed	160 (1.10)	Bundled	275 (1.89)	Proportionate	67.8 (305.1)	63.4 (87.0)
4	Interior	3800 (4140)	26.2 (28.5)	Distributed	160 (1.10)	Distributed	160 (1.10)	Proportionate	69.9 (314.6)	29.9 (41.1)
5	Interior	3600 (4200)	24.8 (28.9)	Distributed	160 (1.10)	Distributed	160 (1.10)	Shear constant at dead load, moment increased to failure	25.2 (113.4)	99.0 (135.9)
6	Interior lift slab	3000	20.7	Bundled	160 (1.10)	Distributed	160 (1.10)	Proportionate	64.0 (288.0)	78.0 (107.1)

*Values in parentheses are top column strengths.

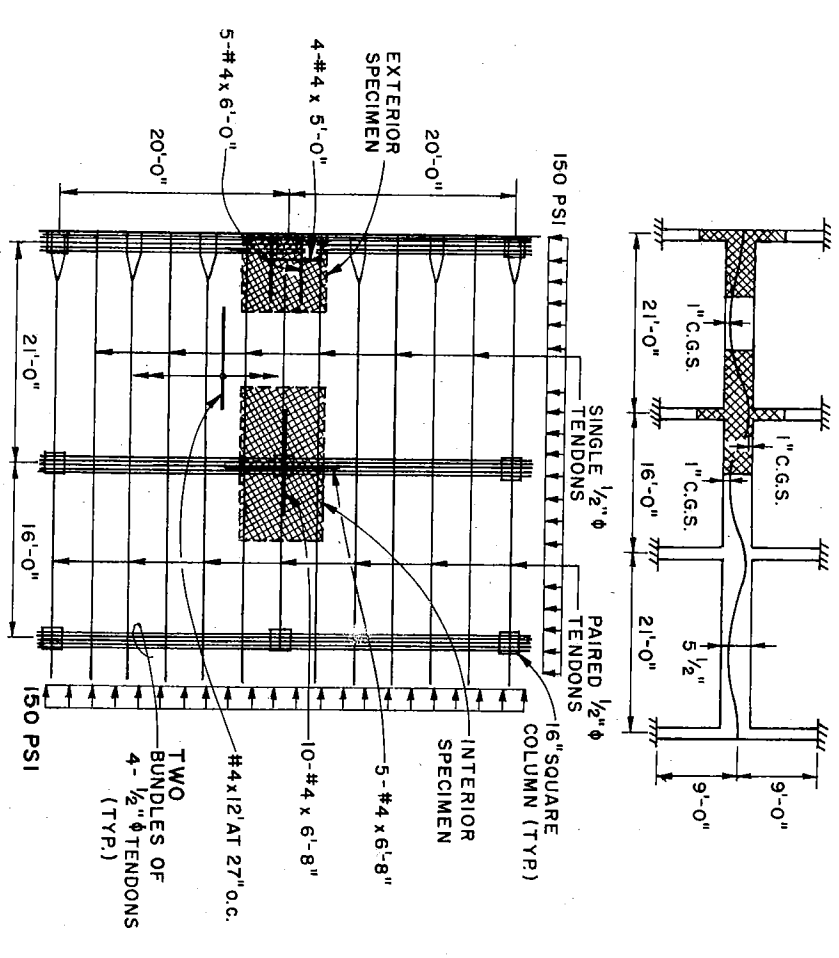

Fig. 1. Layout of prototype structure.

superimposed dead load of 15 psf (720 Pa).

Square columns [16 in. (406 mm)] were needed for shear and a 5.5 in. (140 mm) thick slab prestressed biaxially to 150 psi (1.03 MPa) for stiffness. Tendons were banded through the column in the 20-ft (6 m) direction. To provide the required ultimate flexural capacity and better distribute cracking, additional bonded reinforcement was specified in accordance with ACI 318-77, Section 18.9.3.3.

The proportions, loading, and prestressing for the test specimens were chosen so that the stress and deformation conditions for their slab-column connections closely simulated those likely for the connections in the prototype structure. The test specimens represented to full scale the hatched areas of Fig. 1. All specimens had columns extending 48 in. (1.22 m), above and below the slab, a distance equal to approximately one-half the story height for the prototype structure.

Test Program

The test program is summarized in Table 1. Five interior column-slab subassemblages, including one lift slab specimen, and one exterior column-slab subassemblage, were tested. Plan, longitudinal, and transverse section details for the exterior column specimen 2 are shown in Fig. 4; plan and longitudinal

section details for the typical interior column specimen 1 in Fig. 2; and plan details for the lift slab specimen 6 in Fig. 3.

For cast-in-place connections, the 16-in. (40 mm) square columns of the prototype structure were reduced to 14 in. (356 mm) in order that shear rather than flexural effects would govern according to ACI 318-77. Comprehensive details concerning the design, construction, and testing of the specimens are given in Reference 3.

Interior Column Specimens

As apparent from Table 1, major variables for the interior column cast-in-place specimens were the tendon layout and the loading history. As shown in Fig. 2 for the moment transfer direction of Specimen 1, there were two ½-in. (13 mm) diameter tendons fully stressed to 25 kips (112 kN), through the column, and two ½-in. (13 mm) tendons stressed to 12.5 kips (56 kN), located 6 in. (152 mm) from the edge of the slab. Those tendons were anchored off against steel spreader beams whose reaction points ensured a uniform 160 psi (1.10 MPa) axial compressive stress in the slab for distances more than 15 in. (381 mm) from the slab edge. In Table 1, that type of layout with tendons at 3-ft (0.9 m) centers outside the column is described as distributed.

In the transverse direction, tendons were bundled in two groups of four each and all were equally stressed to 16 kips (72 kN). Those tendons were anchored off against steel spreader beams whose reaction points ensured a uniform 160 psi (1.10 MPa) axial stress in the transverse direction for distances more than about 24 in. (610 mm) from the slab edge. Teflon bearing pads were placed beneath the reactions of the steel spreader beams in order that the stiffness of those beams had minimal effect on the moment transfer characteristics of the subassemblage. In Table 1, the type of layout with eight tendons banded through the column is termed "bundled."

Locations for the top bonded reinforcing bars of Specimens 1, 4, and 5 are indicated by broken lines in Fig. 2. The same amounts of reinforcement were used for all three specimens. The amount within lines one and one-half slab thickness either side of the column was 10 percent less than that required by Eq. (18-7) of ACI 318-77. Outside of

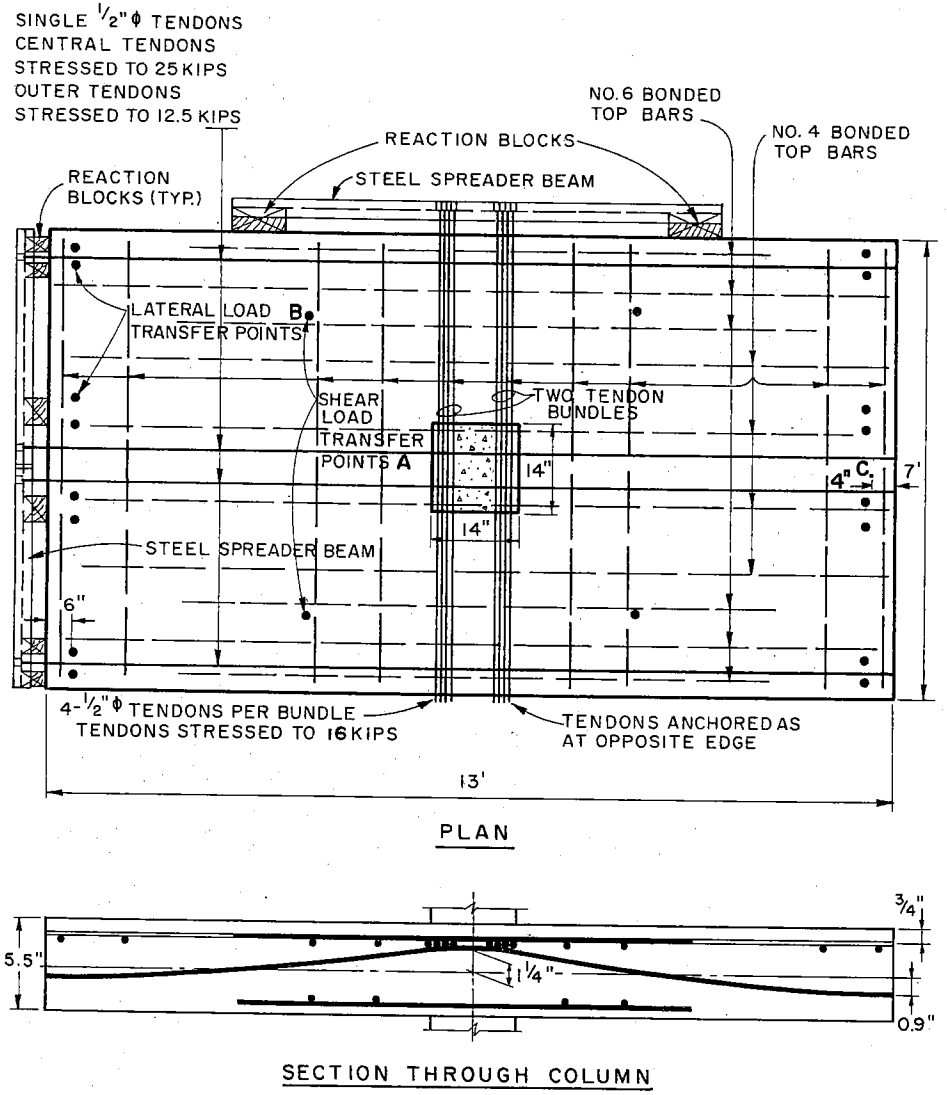

Fig. 2. Properties of typical specimen 1.

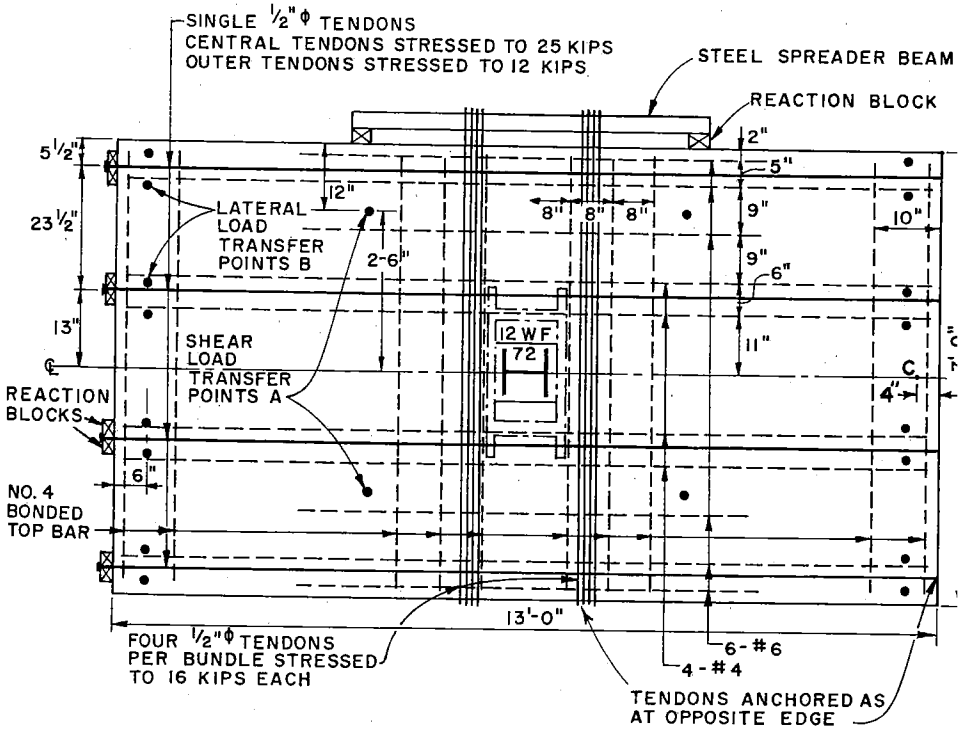

Fig. 3. Properties of lift slab specimen.

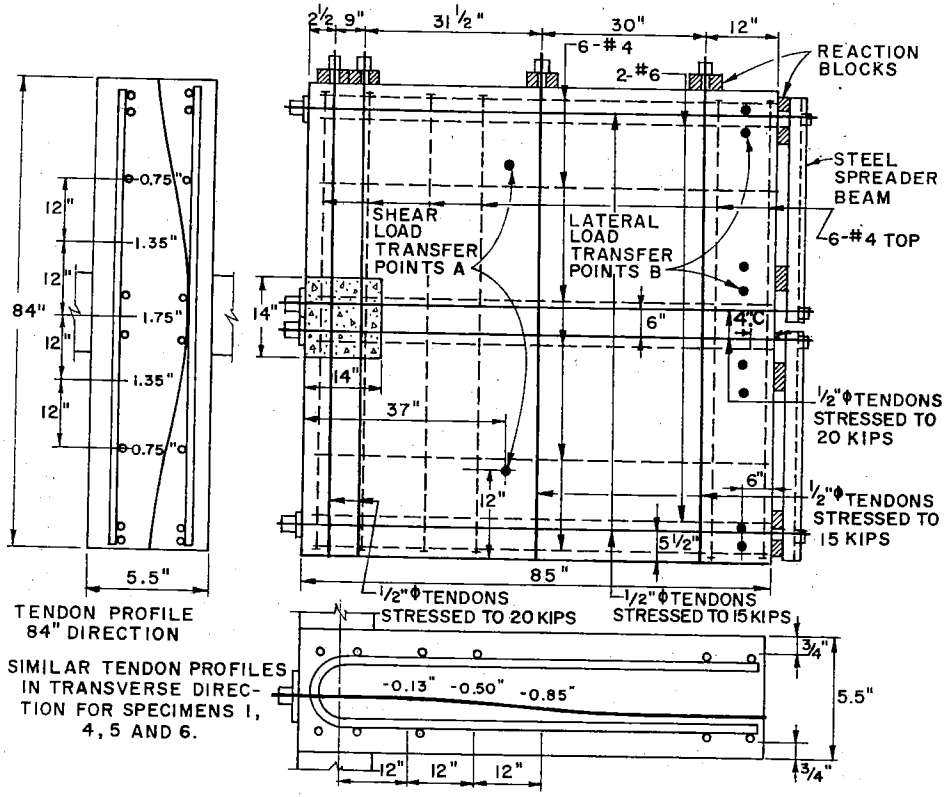

Fig. 4. Properties of edge column specimen.

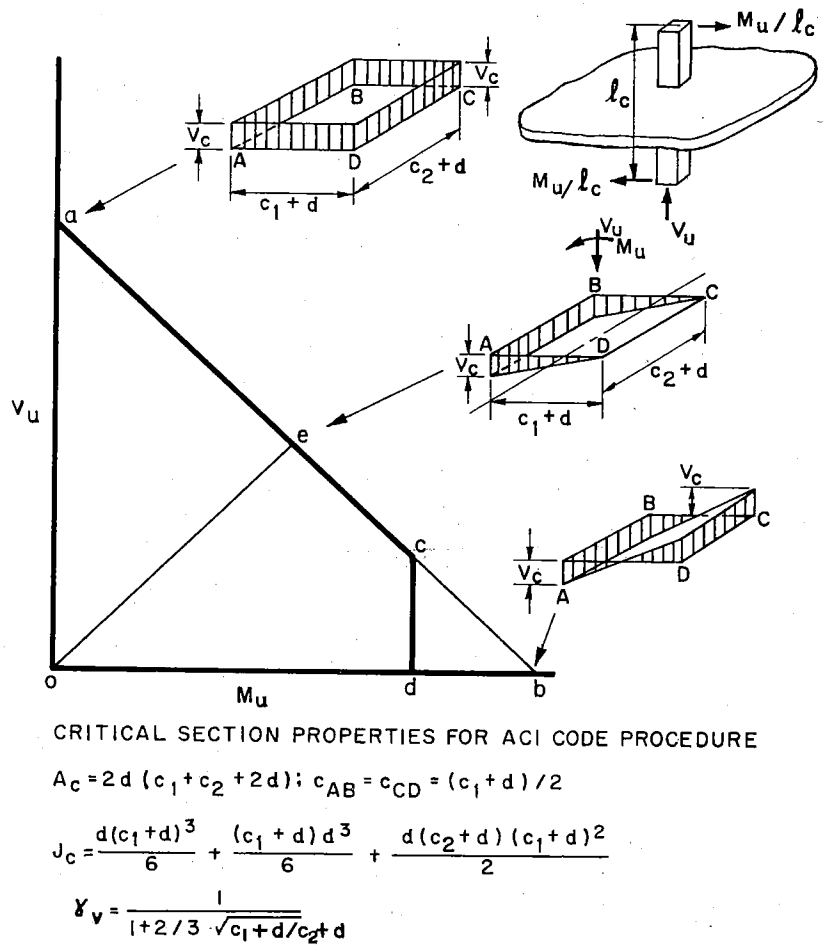

Fig. 5. Moment-shear interaction diagram per ACI 318-77.

the central region, additional bonded bars provided a flexural capacity for the slab equal to the negative moment flexural capacity center-to-center of panels for the prototype structure.

Bottom-bonded reinforcement consisted of two No. 4 bars in each direction through the column and another two No. 4 bars in each direction within one slab thickness either side of the column. Because tendons were bundled in the direction of moment transfer for Specimen 3, two of the No. 6 top bars were replaced with No. 4 bars.

Lift Slab Specimen

Plan details for this specimen are shown in Fig. 3. Lifting collar details are reported in References 3 and 4. The collar was turned so that its larger dimension was in the transverse direction of the slab. A 10 WF 72 steel section was used for the column. In the transverse direction of the slab, the bundled tendons were located outside the lifting collar, but two No. 4 bars lay over the edges of the shearhead arms. Two longitudinal tendons and two No. 4 bars passed over the ends of the shearhead arms. In all other details, the lift slab specimen was constructed similarly to Specimen 1.

Edge Column Specimen

Plan, longitudinal, and transverse section details for this specimen are shown in Fig. 4. Considerations identical to those for the other specimens dictated the column size, tendon profiles, and tendon forces. The amount of bonded reinforcement in the column region was reduced to half that for other specimens in order to examine the effect of that variable. At the edge of the specimen modeling the discontinuous edge of the prototype structure, the tendons were anchored against steel plates in order to replicate the restraint conditions for an actual structure.

Materials

The ½-in. (13 mm) diameter plastic sheathed prestressing tendons had an ultimate strength of 41.1 kips (185 kN) and a yield strength at a 1 percent strain of 37.5 kips (169 kN). The No. 4 and No. 6 bonded reinforcing bars had yield strengths of 66.0 and 66.6 ksi (455 and 459 MPa), respectively. The yield strength of the 4-in. (102 mm) channels used for the shearhead was 49.0 ksi (338 MPa).

The lower column and the slab were cast at one time from one batch of concrete. The upper column was cast 1 to 3 days after the slab. The strength for that concrete is listed in parenthesis in Column 3 of Table 1. The grout between

the steel column and the lifting collar had a strength of 7140 psi (49 MPa) at the time of test of the lift slab specimen.

Test Setup and Instrumentation

The shear force acting on the connection was simulated by jack forces that applied equal loads at Points A in Figs. 2, 3, and 4. Moment transfer was caused by other jack forces that applied equal loads at Points B in Figs. 2, 3, and 4. The jack forces B acted in opposite directions for opposite ends of the slab-interior column specimens. The forces applied at Points A and B are termed the gravity and lateral loads, respectively. The column was held in place at its top by tie rods and pinned at its base.

All specimens were instrumented to provide detailed data on their behavior throughout their entire loading history. Load cells were used to measure the level of prestress in the tendons during prestressing and testing, and the jack forces applied to the slab. A combination of linear potentiometers and deflection scales were used to measure the deflected profile of the surface of the slab, the rotations of the slab with respect to the column over a length equal to the slab depth at the column face, and the column rotations. Electrical resistance strain gages were used to measure strains at selected locations on the bonded reinforcing bars of the slab for all specimens and the lifting collar of the lift slab specimen.

For all interior column specimens except Specimen 5, the line ABCDEFJ in Fig. 6 indicates the overall loading history. Points A, D, etc., correspond to the loading conditions for the prototype structure shown in the Table in Fig. 6. In order to obtain some information on likely seismic effects, the forces transferred to the column were cycled three times over the ranges indicated by the broken lines ED′ and EE′. Reversals between E and D′ yielded information on vertical acceleration effects while reversals between E and E′ yielded information on horizontal acceleration effects. For Specimen 5, the shear was increased until at Point A it equaled the dead load shear, center to center of panels for the prototype structure. Then, as indicated by the broken line AP, the moment transferred to the column was increased until failure occurred. Information on likely seismic effects was again obtained by reversing the moments three times over the ranges JJ′ and KK′.

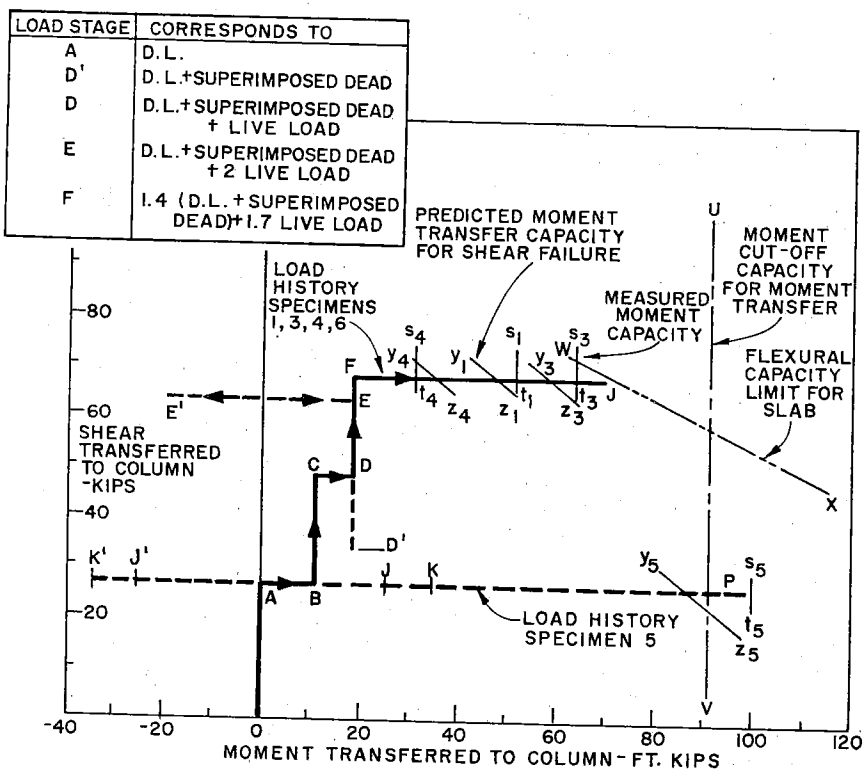

Fig. 6. Load history and measured and computed strengths for interior column specimens.

In practice, the load history for a lift slab connection would differ from that for a cast-in-place connection since the self weight of the slab would not cause moment transfer. However, to simplify comparisons, the load history for the lift slab specimen was made the same as that for Specimen 1 with essentially the same tendon layout. The actual load history for the lift slab specimen is shown in Fig. 7. There are only minor differences between that history and the idealized history shown in Fig. 6. That result is typical of the load histories for the four cast-in-place interior column specimens.

The idealized loading history for Specimen 2 is represented by the line OADH in Fig. 8a. To obtain information on likely seismic effects, the forces transferred to the column were cycled three times between the conditions for Points D and B in Fig. 8a, and three times between conditions for Points F and G. The second variation was produced by holding the forces applied at Points A in Fig. 4 constant and varying only the loads applied at Points B.

For the cast-in-place interior column specimens residual shear capacity tests were made after punching failures had been obtained in the moment transfer tests. With no forces applied at Points B in Fig. 2, the forces at Points A were increased until secondary punching shear failures occurred. Measurements were made of the applied forces, the deflections at the slab edges and the deflection of the slab at a point 2 in. (51 mm) from the column face and in the region of the moment transfer punching failure.

Test Results

This section discusses the load-deflection relationships of the various specimens, the lateral load stiffness, the moment transfer strength, the reinforcement stresses, and the residual shear capacity tests.

Load-Deflection Relationships

Lateral load-edge deflection relationships for the four high shear loading, interior column specimens are shown in Fig. 9. Loads for first cracking of the slab and first yielding of the top bars passing through the column are shown on each diagram. The initial step function form for the response results from the edge deflections increasing when the gravity loads were increased without increase in the lateral loads. The edge deflection is the value measured at Point C in Figs. 2 and 3 where the gravity and lateral forces acted in the same direction for the first application of lateral loading.

For the three cast-in-place connections, large deflections developed prior to failure. However, the lateral load capacity was still increasing rapidly with increasing deflections when punching failures occurred for all three specimens. Only the lift slab specimen

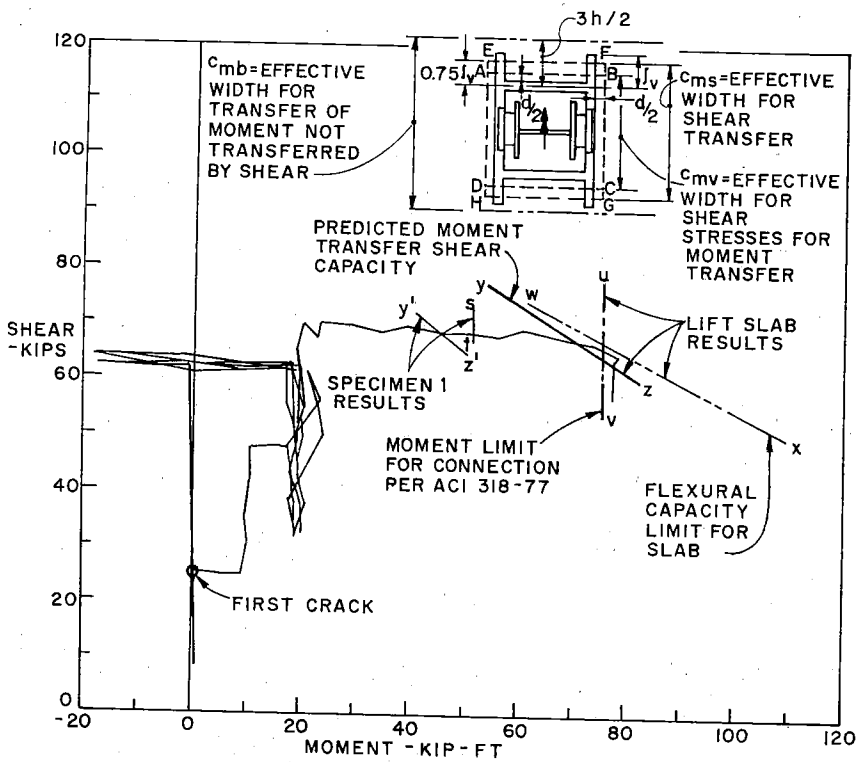

Fig. 7. Load history and measured and computed strengths for lift slab specimen.

exhibited marked plasticity prior to a failure caused by crushing of the concrete beneath one of the reaction blocks for the steel spreader beam.

For the initial lateral loading, the greatest stiffness was shown by Specimen 3 which had tendons bundled through the column in the direction of moment transfer. However, at conditions approaching failure, Specimen 3 showed larger increases in deflection with increasing load than Specimen 1. In that range, most of the increase in moment transfer resistance is provided by the slab sections framing into the side faces of the column. For Specimen 1, with tendons bundled through those side faces, the increase in resistance for a given twist would be larger than for Specimen 3 with distributed tendons in that direction.

The energy dissipation with lateral load cycling was greatest for Specimen 4 and least for Specimen 3. For all three cast-in-place connections, the width of the hysteresis loops decreased rapidly with cycling. The non-yielding, post-tensioning tendons caused elastic recovery effects in spite of yielding of the bonded top bars passing through the column. To obtain reasonable hysteretic damping in seismically loaded prestressed concrete structures, there must be a careful balancing of the amounts of prestress and reinforcing bars in the hinging region.[5]

For this limited test series, the best balance was provided in Specimen 4 with distributed tendons for both directions of the slab. There was no decrease in energy dissipation with cycling for the lift slab specimen 6 because that dissipation was through yielding at the connection between the steel collar and the steel column. There was little energy dissipation with cycling of the gravity loads.

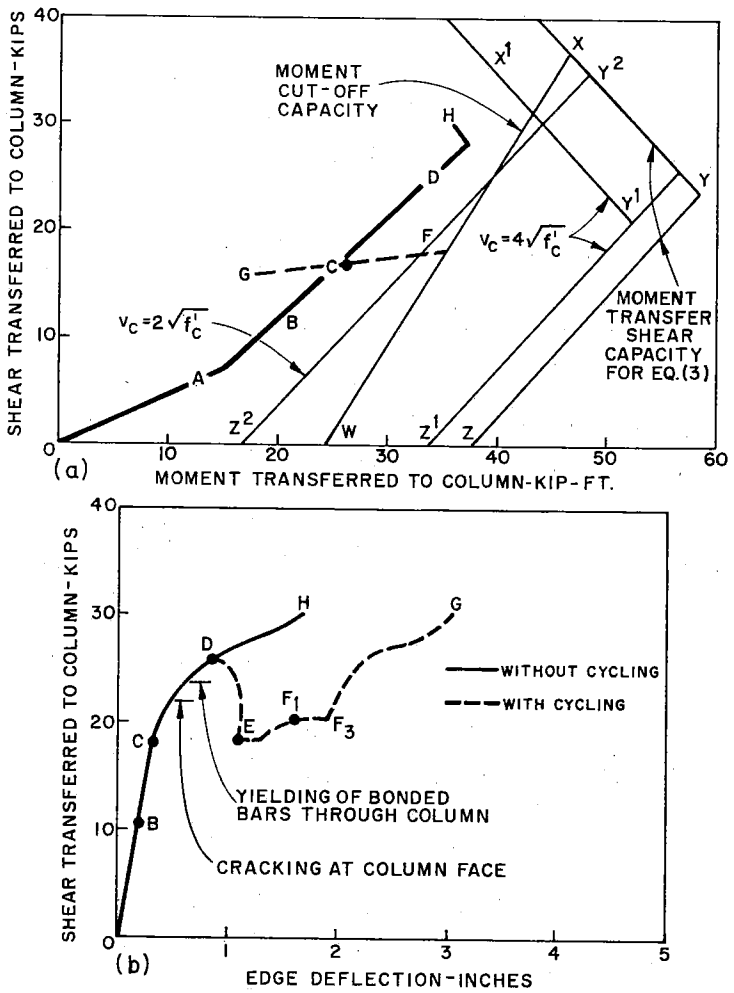

Fig. 8. Load history and load-deflection diagrams for exterior column specimen.

The solid curve in Fig. 10 is the lateral load-edge deflection relationship for Specimen 5. The broken curves are the lateral load-edge deflection envelopes for two comparable reinforced concrete specimens, one without shear reinforcement, S1, and one with integral beam-shear reinforcement, SS2.[6,7] The negative moment flexural capacities on a line extending across the width of the slabs at the column face were comparable for all three specimens and the connections for all three specimens transferred similar gravity load shear forces. However, the columns were 12 in. (305 mm) square for the reinforced concrete specimens.

The reinforced concrete slab without stirrups, S1, failed abruptly in punching shear at a lateral load of 5.5 kips (25 kN). The slab with stirrups had a lateral load capacity of 8.5 kips (38 kN) and developed large deflections prior to the

capacity decreasing with cycling and increasing deflections for deflections in excess of 4 in. (102 mm). Even after significant reversed cyclic loading, the post-tensioned slab still developed an ultimate ductility for uni-directional loading comparing favorably with the reinforced concrete slab with integral beam stirrups.

For the prestressed slab cracking at the column face during the first loading to 2.0 kips (9 kN) resulted in a permanent edge deflection for zero lateral load. For the second and third cycles between lateral loads of 2 kips (9 kN), and for the fourth, fifth, and sixth cycles between lateral loads of 3 kips (13.5 kN), the hysteresis loops remained stable and spindle shaped. Although there was little energy dissipation, there was also no degeneration in stiffness with cycling.

It is apparent that prestressing can provide an excellent means for tying a slab together and ensuring ductile behavior for high intensity wind loadings. The stable reversed cyclic loading characteristics of these slab-interior column subassemblages also suggests that with proper detailing, post-tensioned unbonded slabs will perform satisfactorily under seismic loadings. However, reversed cyclic loading tests of higher intensity than those reported here are necessary to validate that potential and develop the understanding necessary to ensure ductile behavior for intense seismic loading.

The broken curve in Fig. 8b is a plot of the shear transferred to the column (the sum of the gravity and lateral load effects) versus the edge deflection envelope for the slab-exterior column subassemblage. The deflection is that measured at Point C, midway along the length of the interior edge of the slab, in Fig. 4. Although the forces transferred to the column were the same for load stages C and E, permanent deflections developed when cycling of the gravity loads caused the shear to vary between the values for Points D and B in Fig. 8b.

Similarly, the increase in deflection from F1 to F3 indicates the damage caused by cycling the lateral loads between the values for Points G and F in Fig. 8a. The solid curve in Fig. 8b is the response when the damage caused by cycling is deducted from the measured response. The difference between the solid and broken curves indicates the intensely damaging effects of cycling. Torsional cracking developed at the slab edge modeling the discontinuous edge of the prototype structure during the first cycle-to-load stage D. Those cracks opened significantly during the cycling between Stages B and D. After completion of the three load cycles between Stages F and G, those torsional cracks were 0.2 in. (5 mm) wide and the bonded top reinforcing bars passing through the column were yielding.

Tests on reinforced concrete slab-exterior column subassemblages similar to the prestressed subassemblage reported here have shown that torsional cracking develops at a discontinuous edge when the upward shear stress reaches about $2\sqrt{f'_c}$ psi ($0.17\sqrt{f'_c}$ MPa). Unless vertical reinforcement is provided at that edge with a spacing not greater than about 0.75 times the depth of the slab, those torsional cracks open wide with cycling. In a reinforced concrete slab some restraint to that opening is provided when the flexural bars of the slab are hooked at that edge. A prestressed slab lacks even that restraint unless additional hooked bars are provided.

Lateral Load Stiffness

It can be seen from Fig. 6 that for the cast-in-place interior column connections, information on the lateral load stiffness can be obtained by analyzing the response of Specimens 1, 3, and 4 for the load stages AB and CD, and Specimen 5 for load stages A through K.

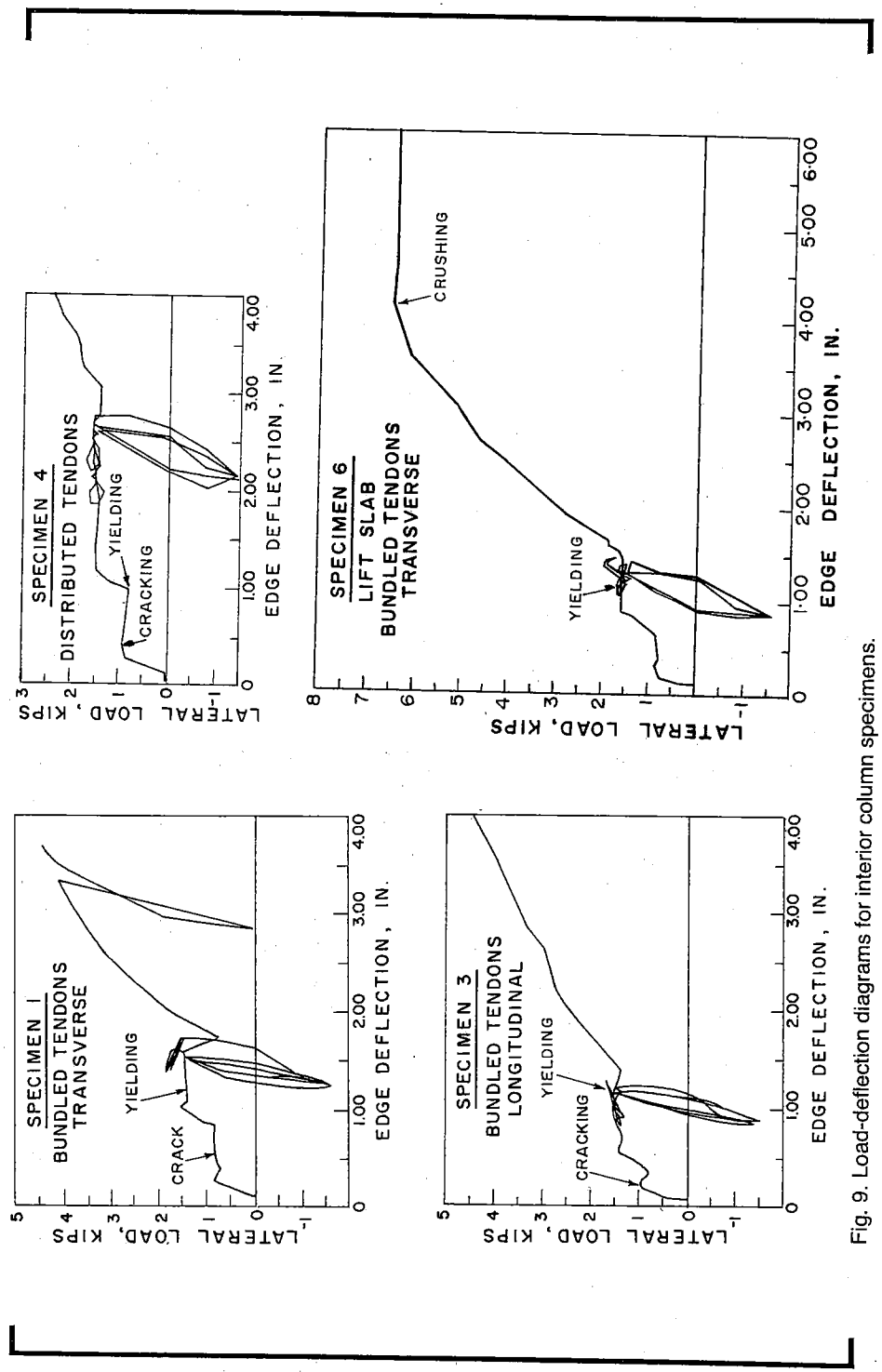

Fig. 9. Load-deflection diagrams for interior column specimens.

For the 0 to 1.0-kip (4.5 kN) lateral load range, the measured stiffnesses varied widely between specimens. For the 1.0 to 2.0-kip (4.5 to 9.0 kN) range, values were essentially the same for all four specimens. For the 0 to 1.0-kip (4.5 kN) range, measured stiffnesses expressed as the lateral load divided by the edge deflection were 16.6, 8.7, 6.3, and 5.5 kips/in., (2.9, 1.5, 1.1, and 1.0 kN/mm) for Specimens 3, 1, 5 and 4, respectively.

Those variations are consistent with the tendon layouts. The high value was for the specimen with tendons bundled in the longitudinal direction, and the next highest value for the specimen with tendons bundled in the transverse direction. For the 1.0 to 2.0-kip (4.5 to 9.0 kN) lateral load range, all slabs were visibly cracked in the column region and the lateral load stiffness was 3.8 kips/in. (0.67 kN/mm). The measured stiffness for Specimen 3 for the 0 to 1.0-kip (4.5 kN) range was consistent with the value predicted using the provisions of Section 13.7 of ACI 318-77, assuming the slab to be uncracked.

The observed contributions of slab bending and torsional rotations to the measured edge deflections were also consistent with the ACI Code provisions. For the 1.0 to 2.0-kip (4.5 to 9.0 kN) range, the measured stiffness of 3.8 kips/in. (0.67 kN/mm) was consistent with the value predicted assuming the slab to be cracked in bending and the torsional stiffness to be one-tenth of that predicted using Eq. (13-7) of ACI 318-77. The observed contributions of slab bending and torsional rotations were then consistent with code provisions. When that torsional stiffness reduction was also used for the 0 to 1.0-kip (4.5 kN) range, but the slab assumed to be uncracked in bending, the predicted stiffness was about 6.5 kips/in. (1.15 kN/mm). That value is consistent with the measured stiffnesses of Specimens 1, 4, and 5 for that range.

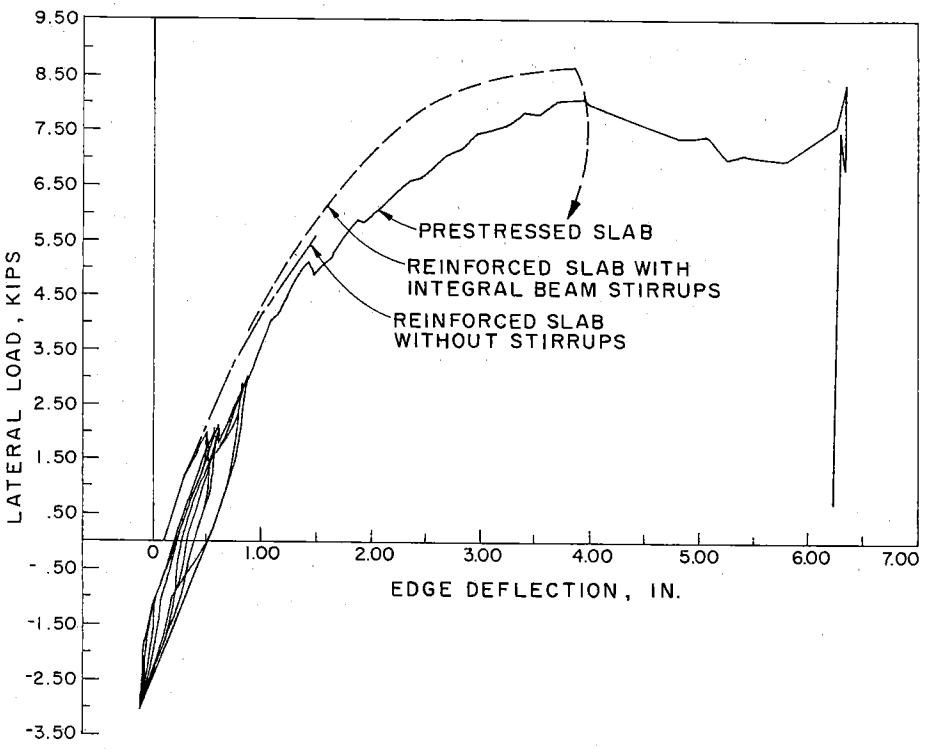

Fig. 10. Comparison of load-deflection diagrams for reinforced and prestressed concrete subassemblages.

Because of the manner in which prestressed slabs are designed, it is difficult to predict when cracking will occur in a prototype structure. The lateral load response of these specimens was obviously sensitive to cracking and stiffnesses dropped even before cracking was detected. Further investigations of lateral load stiffness are needed. In the interim, these results suggest that for high levels of prestress in the direction of moment transfer, the slab can be taken as uncracked and the lateral load stiffness assessed using ACI 318-77, Section 13.7 provisions. If, however, the level of prestress is low, the slab should be assumed to be cracked in bending and the torsional stiffness taken as one-tenth that predicted by Eq. (13-7) of ACI 318-77.

Moment Transfer Strength

ACI Code 318-77 provisions define a moment-shear interaction diagram for interior column connections having the form shown in Fig. 5. For all connection types, Section 11.12.2 requires that shear stresses on a critical section located $d/2$ from the column perimeter be calculated from the formulas:

$$v_{u(AB)} = \frac{V_u}{A_c} + \frac{\gamma_v M_u c_{AB}}{J_c} \qquad (1)$$

or

$$v_{u(CD)} = \frac{V_u}{A_c} - \frac{\gamma_v M_u c_{CD}}{J_c} \qquad (2)$$

where $\gamma_v M_u$ is the fraction of the total moment M_u transferred by shear across the critical section, A_c and J_c are the area and polar moment of inertia of the critical section, and M_u is the moment acting about the centroid of the critical section and to be transferred to the column.

For the interior column connection shown in Fig. 5 $|v_{u(AB)}|$ is always greater than $|v_{u(CD)}|$. Line ab in Fig. 5 represents the condition where $v_{u(AB)}$ is limited to some constant maximum shear stress, v_c. The diagrams on Fig. 5 indicate shear stress distributions for various points along ab. Section 13.3.4 of ACI 318-77 requires that reinforcement be provided within lines one and one-half times the slab thickness either side of the column to transfer the fraction of the moment $(1 - \gamma_v) M_u$ not transferred by shear. If there is insufficient reinforcement, the moment cut-off, cd, in Fig. 5 results. For an exterior column connection, the centroid of the critical section lies further from the slab edge than the centroid of the column so that $|v_{u(CD)}|$ can be greater than $|v_{u(AB)}|$ when M_u is large. In that case a second shear limitation line, such as YZ in Fig. 8a, results.

Based on a review of available test data, ACI-ASCE Committee 423[8] has recommended that Eq. (11-13) of ACI 318-77 be used to determine the shear strength of connections transferring shear only. For slabs Eq. (11-13) becomes:

In U.S. units:

$$v_c = 3.5\sqrt{f'_c + 0.3 f_{pc} + V_p/A_c} \geq 4\sqrt{f'_c \text{ psi}} \qquad (3a)$$

and in SI units:

$$v_c = 0.3\sqrt{f'_c + 0.3 f_{pc} + V_p/A_c} \geq 0.34\sqrt{f'_c \text{ MPa}} \qquad (3b)$$

where f_{pc} is the axial prestress in the slab and V_p is the sum of the vertical components of all prestressing tendons crossing the critical section for shear.

Shown in Fig. 6 is the correlation between measured and predicted strengths for the cast-in-place interior column specimens. The line UV on the

right of Fig. 6 corresponds to line cd in Fig. 5 and indicates the moment cut-off capacity for Specimens 1, 4, and 5. The reinforcement effective for moment transfer was taken as four No. 4 top bars, four No. 4 bottom bars, and two tendons stressed to 25 kips (112 kN) each. For Specimen 3, line UV would be further to the right due to the larger number of longitudinal tendons. The sloping line, WX, on the right of Fig. 6 indicates the theoretical relationship for the negative moment flexural capacity of the slab of Specimens 1, 4, and 5.

The measured moment capacities for failure for Specimens 1, 3, 4, and 5 are indicated by the vertical lines s_1t_1, s_3t_3, s_4t_4, and s_5t_5 crossing the load history lines. The adjacent sloping lines y_1z_1, y_3z_3, y_4z_4, y_5z_5 indicate the respective shear capacities when the shear stress calculated from Eq. (1) is limited to the value obtained from Eq. (3) with f_{pc} taken as the axial prestress in the direction of moment transfer. All specimens failed by punching and the measured capacities were slightly greater than the predicted, shear stress limited, moment transfer capacities for all specimens except Specimen 4. Specimen 4 had a capacity only 2 percent less than the predicted capacity.

Shown in Fig. 7 is the correlation between measured and predicted capacities for the lift slab specimen 6. The notation for each line is the same as that for Fig. 6. As recommended in Reference 9, the shear stress caused by moment transfer [second term of Eq. (1)] was evaluated using the critical section ABCD shown on the insert in Fig. 7. The shear stress caused by shear transfer [first term of Eq. (1)] was evaluated using the critical section EFGH. The lift slab specimen failed due to excessive deflections. That behavior was in close agreement with the predicted behavior.

Shown in Fig. 8 is the correlation between the load history for the exterior column specimen 2 and predicted capacities. The sloping lines XY and YZ indicate the limiting capacities when the shear stresses given by Eqs. (1) and (2), respectively, equal the strength calculated from Eq. (3). The sloping line WX indicates the moment cut-off capacity dictated by the reinforcement within lines one and one-half times the slab thickness either side of the column.

It is apparent that the measured strength is over-estimated by those procedures. If the connection is analyzed according to reinforced concrete procedures, the lines X^1Y^1 and Y^1Z^1 result when v_u is limited to $4\sqrt{f'_c}$ ($0.34\sqrt{f'_c}$ MPa) and the line Y^2Z^2 results when v_u is limited to $2\sqrt{f'_c}$ (0.17 MPa) at the discontinuous edge. The specimen failed in punching shear at the front face after the torsional cracks opened wide during the cycling between load stages F and G.

Apparently until further data are available, strengths for prestressed concrete exterior column connections should be evaluated using the procedures for reinforced concrete. Correlations with data for similar reinforced concrete connections[10] show that edge reinforcement, detailed so that it can act as torsional reinforcement, must be provided if the value of v_u given by Eq. (2) is predicted as exceeding $2\sqrt{f'_c}$ (0.17 MPa).

Calculations for comparisons of measured and predicted strengths are summarized in Table 2. The maximum applied stress, calculated from Eq. (1) is listed in Column (5). That value equals the sum of the component stresses listed in Columns (3) and (4). The resisting capacity calculated from Eq. (3) is listed in Column (9). That value equals the sum of the three components listed in Columns (6), (7), and (8). The longitudinal prestress contribution, Column (7), is greater for Specimen 3 than for the other specimens because the bundled strands provided an effective prestress of 275 psi (1.9 MPa) in the direction of moment transfer compared with 160 psi (1.1 MPa) for the other specimens. With draped bundled strands, a shear resistance component V_p/A_c can be provided as large as the component provided by the prestress term $0.3f_{pc}$.

Column (11) lists the fraction of the moment to be resisted by reinforcement within lines one and one-half times the slab thickness either side of the column. The quantity M_r in Column (12) is the capacity of the reinforcement. Moment cut-off failures, rather than punching failures, are predicted for Specimens 5 and 6. That prediction was consistent with the observed behavior.

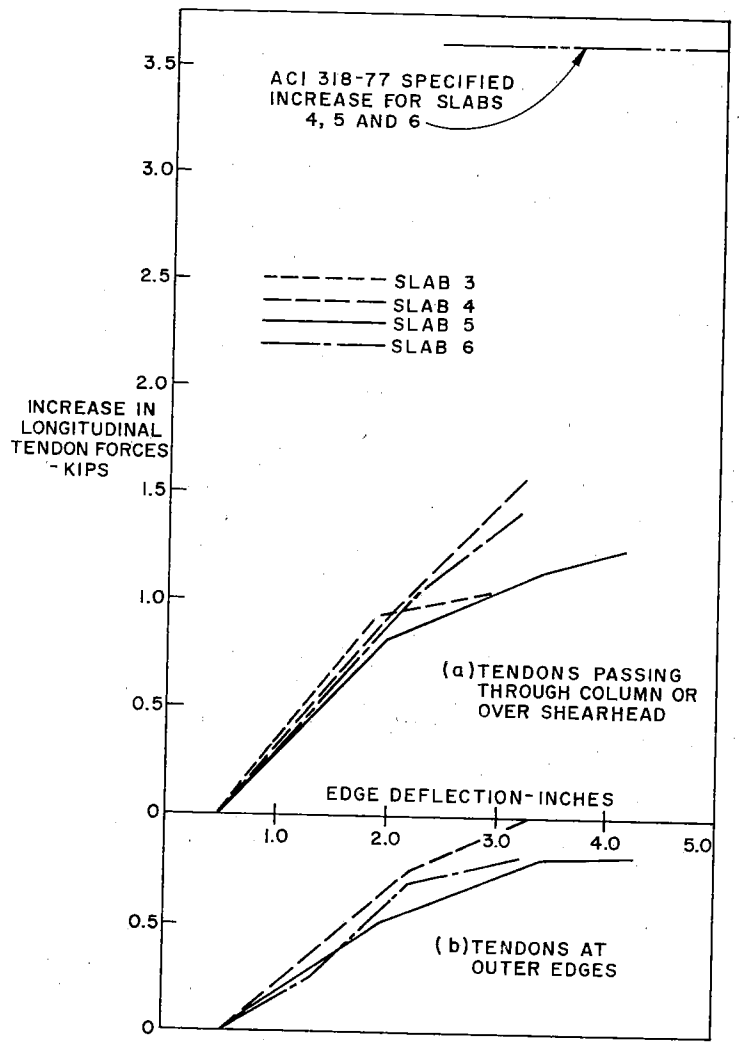

Fig. 11. Increase in forces in longitudinal tendons.

Reinforcement Stresses

Shown in Fig. 11 are the increases in forces in the longitudinal tendons of the

slab for increasing edge deflections. Increases in forces in the transverse tendons did not exceed 0.3 kips (1.35 kN). ACI 318-77 permits the stress in an unbonded tendon at failure to be determined from the formula:
In U.S. units:

$$f_{ps} = f_{se} + 10{,}000 + \frac{f'_c}{100\,\rho_p} \text{ psi} \quad (4a)$$

and in SI units:

$$f_{ps} = f_{se} + 69 + \frac{f'_c}{100\,\rho_p} \text{ MPa} \quad (4b)$$

where f_{se} is the effective prestress and ρ_p the prestressed reinforcement ratio.

Eq. (4) is theoretically applicable to the longitudinal tendons passing through the column of Specimens 4, 5, and 6. The increase in tendon forces predicted by Eq. (4) for those specimens is 3.7 kips (16.6 kN). As indicated in Fig. 11, measured increases were considerably less than that prediction even though the slabs developed large edge deflections prior to failure. It is recommended that for evaluations of moment transfer capacity, no increase in tendon forces be recognized and that use of Eq. (4) be limited to flexural strength evaluations.

For loading conditions to the right of line oe in Fig. 5, upward shear stresses develop at the back face of the column and cracking occurs for reinforced concrete connections when that stress exceeds $0.3\sqrt{f'_c}$ ($0.03\sqrt{f'_c}$ MPa). Bottom reinforcement continuous through the connection area is needed to arrest that cracking. For all the interior column prestressed specimens except Specimen 5, the stresses listed in Column (3) of Table 2 exceed those in Column (4) and therefore according to experience for reinforced concrete, cracking was not to be expected. However, in the tests cracking occurred and significant tensile stresses developed in the bottom reinforcement at the back face of the column.

No simple criterion, such as that for reinforced concrete, could be established for conditions for cracking. For the high moment Specimen 5, the reinforced concrete criterion was satisfactory. However, for the high shear Specimens 1, 3, and 4, cracking apparently occurred as soon as the top steel yielded provided the $\gamma_v M_u c_{CD}/J_c$ term in Eq. (2) exceeded $0.7\sqrt{f'_c}$ ($0.06\sqrt{f'_c}$ MPa).

Further investigations of bottom reinforcement requirements are highly desirable and are recommended.

Residual Shear Capacity

As previously described, residual shear capacity tests were conducted after punching failures occurred in the moment transfer tests. Specimens 1, 3, 4, and 5 had residual capacities of 95.6, 100.6, 93.0, and 87.0 kips (430, 453, 418, and 391 kN), respectively. Those capacities were 92, 90, 98, and 94 percent, respectively, of the shear transfer only capacities predicted using Eq. (3). Specimens 1, 4, and 5 failed explosively when a punching failure completely encircled the column and the concrete beneath the bearing pads for the transverse tendons crushed. Specimen 3 developed a punching failure encircling the column and the slab dropped down the column about 2 in. (50 mm) but did not fail explosively.

The performance of these prestressed slabs in residual shear capacity tests was much better than that of reinforced concrete slabs.[6,7] Residual capacities for reinforced concrete slabs are sensitive to the amount of bonded bottom reinforcement. Unless those slabs contain integral beam shear reinforcement, their residual capacities are about one-half their undamaged shear transfer capacities. Obviously, prestressing is an effective means of tying a slab together and a progressive collapse is unlikely unless tendon anchorage failure occurs or tendons are cut.

Table 2. Comparison of measured and computed strengths.

Specimen	$\sqrt{f'_c}$	Moment transfer shear capacity								Moment cut-off capacity	
		Applied stresses			Resistance components						
		$\frac{V_u}{A_c}$	$\frac{\gamma_v M_u c_{AB}}{J_c}$	v_u^*	$3.5\sqrt{f'_c}$	$0.3 f_{pc}$	$\frac{V_p}{A_c}$	v_c†	v_u/v_c	$(1-\gamma_v)M_u$	Col. (11) / M_r^+ (12)
(1)	(2)	(3)	(4)	(5)	(6)	(7)	(8)	(9)	(10)	(11)	
	psi (MPa)	psi (MPa)	psi (MPa)	psi (MPa)	psi (MPa)	psi (MPa)	psi (MPa)	psi (MPa)		kip-in. (kN-m)	
1	62.0 (0.43)	207 (1.43)	123 (0.85)	330 (2.28)	217 (1.50)	49 (0.34)	53 (0.37)	319 (2.20)	1.03	371 (42.3)	0.60
3	60.4 (0.42)	210 (1.45)	151 (1.05)	361 (2.49)	211 (1.46)	83 (0.57)	52 (0.36)	346 (2.39)	1.04	457 (52.1)	0.65
4	61.6 (0.43)	216 (1.49)	71 (0.49)	287 (1.98)	216 (1.49)	49 (0.34)	28 (0.19)	293 (2.02)	0.98	216 (24.6)	0.34
5	60.0 (0.41)	78 (0.54)	236 (1.63)	314 (2.17)	210 (1.45)	49 (0.34)	28 (0.19)	287 (1.98)	1.09	713 (81.3)	1.11
6	54.8 (0.38)	144 (0.99)	108 (0.75)	252 (1.74)	192 (1.32)	49 (0.34)	41 (0.28)	281 (1.94)	0.90	593 (67.6)	1.06
2	64.8 (0.45)	138 (0.95)	95 # (0.66)	234 (1.61)	227 (1.57)	45 (0.31)	14 (0.10)	286 (1.97)	0.82	190 # (21.7)	0.98

*v_u is evaluated from Eq. (1); # M_u equals the moment acting about the centroid of the critical section.
†v_c is evaluated from Eq. (3); + M_r equals the flexural capacity of reinforcement (top, bottom, and prestress) within lines $3h/2$ either side of the column.

Conclusions

Based on the prestressed concrete test results reported here and their correlation with available data for similar reinforced concrete subassemblages, it is concluded that:

1. The moment transfer capacity of prestressed concrete slab to interior column connections can be evaluated using the procedures of Sections 11.12.2 and 13.3.4 of ACI 318-77. For dense aggregate concretes, the shear stress v_u should not exceed the value of v_c calculated from Eq. (11-13) of the Code expressed in the form of Eq. (3) of this paper. All reinforcement, bonded and unbonded, within lines one and one-half times the slab thickness either side of the column are effective for transferring the portion of the moment not transferred by shear. No increase in unbonded tendons forces should be assumed in calculations of the moment transfer capacity.

2. For prestressed concrete slab to exterior column connections transferring moments normal to a discontinuous edge, bonded reinforcement, detailed so that it can act as torsional reinforcement, should be provided at the discontinuous edge when the shear stress given by Eq. (2) exceeds $2\sqrt{f'_c}$ psi ($0.17\sqrt{f'_c}$ MPa).

3. Tendons bundled through the column or over the lifting collar are an effective means of increasing the moment transfer strength of slab-interior column connections.

4. Bonded top reinforcement of the amount and distribution required by ACI 318-77, Section 18.9.3.3, is desirable, although the width and distribution of cracking is satisfactory for interior connections with 90 percent of the amount of reinforcement required by ACI 318-77.

5. Conclusions 1, 3, and 4 are applicable to lift slab interior column connections.

6. Further investigations of the conditions controlling cracking at the back face of an interior column connection for moment transfer conditions are desirable. In the interim, bonded bottom reinforcement at least equal to that required by ACI 318-77, Section 7.13, should be provided once the shear stress caused by moment transfer, $\gamma_v M_u c_{CD}/J_c$ exceeds $0.7\sqrt{f'_c}$ psi ($0.06\sqrt{f'_c}$ MPa).

7. Further investigations of lateral load stiffness are desirable. In the interim, if the slab has a significant margin of safety against cracking, the lateral load stiffness should be assessed using ACI 318-77, Section 13.7. If, however, that margin is small, the cracked section bending stiffness should be used and the torsional stiffness taken as one-tenth that calculated from Eq. (13-7) of ACI 318-77.

Acknowledgment

Funding for RCRC Project 39 was provided by the Post-Tensioning Institute, the Reinforced Concrete Research Council and the International Lift Slab Companies. The subassemblages were fabricated and tested by James Chen, Narong Trongtham and Daniel Symonds, former graduate students in the Department of Civil Engineering.

* * *

REFERENCES

1. ACI Committee 318, "Building Code Requirements for Reinforced Concrete (ACI 318-77)," American Concrete Institute, Detroit, Michigan, 1977, 102 pp.
2. *Design of Post-Tensioned Slabs*, Post-Tensioning Institute, Phoenix, Arizona, 1977, 52 pp.
3. Trongtham, N., and Hawkins, N. M., "Moment Transfer to Columns in Unbonded Post-Tensioned Prestressed Concrete Slabs," Report SM 77-3, Department of Civil Engineering, University of Washington, Seattle, Washington, October, 1977.
4. Hawkins, N. M., and Trongtham, N., "Moment Transfer Between an Unbonded Post-Tensioned Prestressed Concrete Lift Slab and Column," Report to International Lift Slab Corporation, November, 1977.
5. Hawkins, N. M., "Seismic Resistance of Prestressed and Precast Concrete Structures" (Parts 1 and 2), PCI JOURNAL, V. 22, No. 6, November-December, 1977, pp. 80-110; V. 23, No. 1, January-February, 1978, pp. 40-58.
6. Hawkins, N. M., Mitchell, D., and Sheu, M. S., "Reversed Cyclic Loading Behavior of Reinforced Concrete Slab Column Connections," *Proceedings*, U.S. National Conference on Earthquake Engineering, Ann Arbor, Michigan, June, 1975.
7. Hawkins, N. M., Mitchell, D., and Hanna, S. N., "The Effects of Shear Reinforcement on the Reversed Cyclic Loading Behavior of Flat Plate Structures," *Canadian Journal of Civil Engineering*, V. 2, December, 1975.
8. ACI-ASCE Committee 423, "Tentative Recommendations for Prestressed Concrete Flat Plates," *ACI Journal*, V. 17, No. 2, February, 1974.
9. Hawkins, N. M. and Corley, W. G., "Moment Transfer to Columns in Slabs with Shearhead Reinforcement," *Shear in Reinforced Concrete*, SP-42, V. 2, American Concrete Institute, Detroit, Michigan, 1974.
10. Hawkins, N. M., Wong, C. F., and Yang, C. H., "Slab-Edge Column Connections Transferring High Intensity Reversing Moments Normal to the Edge of the Slab," Report SM 77-1, Department of Civil Engineering, University of Washington, May, 1978.

* * *

NOTE: A Notation section is given on the following page.

Discussion of this paper is invited. Please forward your comments to PCI Headquarters by September 1, 1981.

APPENDIX—NOTATION

A_c = area of concrete of assumed critical section for transfer of moment at slab-column connection (Fig. 5)

c_1 = size of rectangular or equivalent rectangular column measured in direction of span for which moments are being determined (Fig. 5)

c_2 = size of rectangular or equivalent rectangular column measured transverse to direction of span in which moments are being determined (Fig. 5)

c_{AB}, c_{CD} = distance from centroid axis of assumed critical section to faces AB, CD of critical section (Fig. 5)

c_{mb} = effective width of assumed critical section measured transverse to direction of span in which moments are being determined and within which reinforcement is effective for transfer of fraction of moment not transferred by shear stresses (Fig. 7)

c_{ms} = effective width of assumed critical section measured transverse to direction of span in which moments are being determined, for calculation of shear stresses caused by shear transfer in a connection with shearhead reinforcement, (Fig. 7)

c_{mv} = effective width of assumed critical section, measured transverse to the direction in which moments are being determined, for calculation of shear stresses caused by transfer of moment at a connection with shearhead reinforcement (Fig. 7)

d = distance from extreme compression fiber to centroid of longitudinal tensile reinforcement at perimeter of critical section for shear transfer

f'_c = compressive strength of concrete

f_{pc} = resultant compressive stress at centroid of cross section (after allowance for all prestress losses) in the direction of the span for which moment transfer effects are calculated

f_{ps} = stress in prestressed reinforcement at nominal strength

f_{se} = effective stress in prestressed reinforcement (after allowance for all prestress losses) in direction of span for which moment transfer effects are calculated

h = overall thickness of slab

J_c = property of assumed critical section analogous to polar moment of inertia (Fig. 5)

l_v = length of shearhead arm from centroid of concentrated load or reaction

M_r = moment resistance for transfer of moment that can be contributed by reinforcement (top, bottom, and prestress), within lines $3h/2$ either side of column

M_u = moment to be transferred to column

v_c = permissible shear stress that can be carried by concrete [Eq. (3)]

v_u = shear stress at critical section [Eqs. (1) and (2)]

V_p = vertical component of total effective prestress force at perimeter of critical section

V_u = shear force to be transferred to column

γ_v = fraction of unbalanced moment transferred by eccentricity of shear at slab-column connection

ρ_p = ratio of prestressed reinforcement

* * *

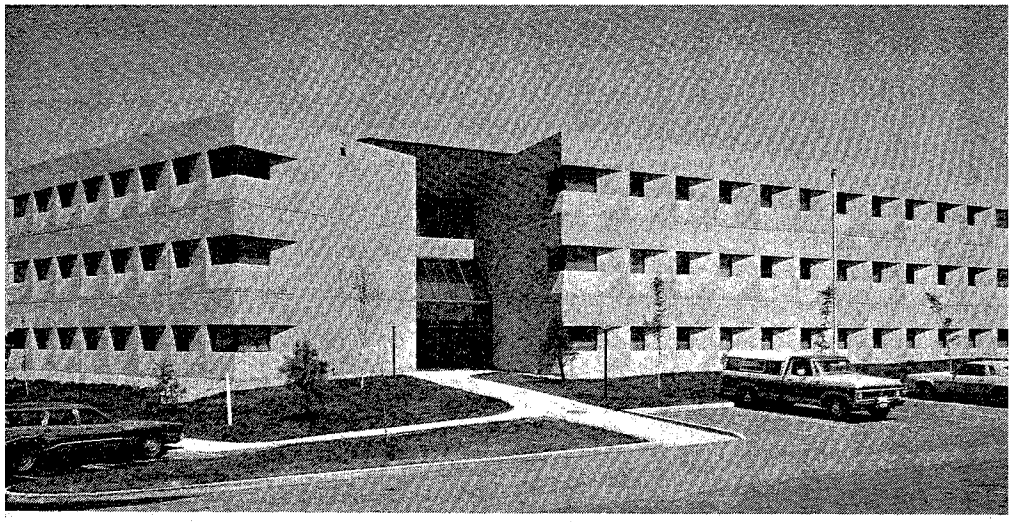

Greenwood Medical Building, Arapaho County, Colorado—The recessed window area and thermal mass of the architectural precast concrete wall panels on this building work in combination to create an efficient passive solar energy system. The designers made full use of standard precast prestressed concrete components in the structural system by incorporating a 32 x 32 ft. (10 x 10 m) structured bay throughout the building. Included in the totally precast structural system are double-tee floor and roof slabs, inverted tee beams, ledger beams, rectangular beams, and interior columns. Cantilevered double-tee floor units add circulation space to a central atrium.

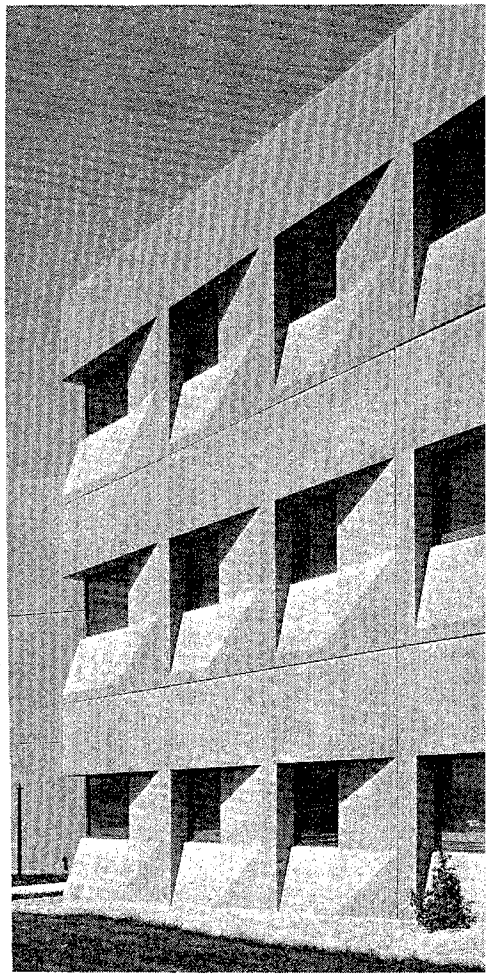

Architect:
Ohlson Lavoie Corporation,
Denver, Colorado.

Structural Engineer:
Borman/Smith & Partners,
Denver, Colorado.

General Contractor:
Penner Construction Management,
Denver, Colorado

Precast Prestressed Manufacturer:
Stanley Structures,
Denver, Colorado.